

Cyclic peptide models of the Ca^{2+} -binding loop of α -lactalbumin

Viktor Farkas,^a Elemér Vass,^a Ignace Hanssens,^b Zsuzsa Majer^{a,*} and Miklós Hollósi^a

^aDepartment of Organic Chemistry, Eötvös Loránd University, PO Box 32, H-1518 Budapest 112, Hungary

^bInterdisciplinary Research Center, K.U. Leuven Campus Kortrijk, B-8500 Kortrijk, Belgium

Received 3 May 2005; revised 8 June 2005; accepted 9 June 2005

Available online 19 July 2005

Dedicated to Professor Koji Nakanishi, a pioneer of biomolecular chemistry, who was awarded the 2004 Tetrahedron Prize.

Abstract—A series of cyclic peptides with different linkers were designed and synthesized to model the elbow-type Ca^{2+} -binding loop of α -lactalbumin (LA). All amino acids of the Ca^{2+} -binding loop are strikingly well conserved among LAs of different species with the sequence Lys⁷⁹-Phe-Leu-Asp⁸²-Asp-Asp-Leu-Thr-Asp⁸⁷-Asp⁸⁸, where three carboxylates of Asp⁸², Asp⁸⁷, and Asp⁸⁸ and the amide carbonyl oxygen atoms of Lys⁷⁹ and Asp⁸⁴ participate in Ca^{2+} binding. Alanine-containing models were also prepared for monitoring the role of the binding (82, 87–88) and nonbinding Asp residues (83–84) in coordinating the cation. The structural features of synthetic peptides and their Ca^{2+} -binding properties were investigated in solution by circular dichroism (CD) and Fourier transform infrared (FTIR) spectroscopy. In water, the CD curves show a strong negative band below 200 nm as a sign of the presence of unfolded conformers. In TFE, all cyclic peptides were found to have a CD spectrum, reflecting the presence of folded (turn) conformers. The effect of Ca^{2+} was dependent on the structure and concentration of the model and the Ca^{2+} to peptide ratio (r_{cat}). A surprising time dependence of the FTIR spectra of Ca^{2+} complexes of the Ala-containing peptides was observed. The shape of the broad amide I band showed no more change after ~60 min. Contrary to this, the deprotonation of the side chain COOH group(s) and formation of the final coordination sphere of Ca^{2+} took more time. Infrared spectra showed that in the Ca^{2+} complex of model comprising the binding Asp residues of LA, the cation is coordinated to the COO[−] groups of all three Asps, while in the complex of model comprising nonbinding Asp residues of LA, the two neighboring Asp side chains form a bridged Ca^{2+} -binding system.

© 2005 Elsevier Ltd. All rights reserved.

1. Introduction

The strong and selective binding of Ca^{2+} to a large number of proteins is closely related to the regulation of many physiological functions. A good understanding of the selective impact of Ca^{2+} essentially implies the unraveling of determinants that contribute to Ca^{2+} affinity. Rationally designed low-molecular-weight model compounds that contain the key ligand amino acids are very useful in such study. In this article, we focus on determining the importance of conservative amino acids within the Ca^{2+} -binding loop of α -lactalbumins (LAs).

Since it was found that α -LA binds Ca^{2+} ,¹ there has been a thorough investigation of the physicochemical aspects of the metal binding to the protein.² Calcium

binding stabilizes the native state of LA in such a way that, for instance, the temperature induced unfolding of an LA shifts from near 20 °C for the apo-protein to nearly 70 °C for the Ca^{2+} -bound protein.³ Moreover, correct refolding and correct disulfide repairing of the reduced LA requires the presence of Ca^{2+} .⁴ The crystallographic analysis of the structure of LA^{5,6} revealed an extremely well-formed Ca^{2+} -binding loop that differs from the EF-hand Ca^{2+} -binding loops.⁷ It has been termed ‘the elbow Ca^{2+} -binding loop’ (Fig. 1). The loop consists of 10 amino acid residues. In most LAs, it extends from Lys⁷⁹ to Asp⁸⁸ and consists of the sequence Lys⁷⁹-Phe-Leu-Asp⁸²-Asp-Asp-Leu-Thr-Asp⁸⁷-Asp⁸⁸. Five residues contribute to liganding Ca^{2+} : three carboxylates of Asp⁸², Asp⁸⁷, and Asp⁸⁸ and two peptide carbonyl oxygen atoms of Lys⁷⁹ and Asp⁸⁴. The very slightly distorted pentagonal bipyramidal metal coordination is completed by two additional water molecules. The elbow Ca^{2+} -binding loop is flanked by a short 3_{10} -helix at the N-terminal side and an α -helix at the C-terminal side. Both structures contribute to orienting the amino acid side chains of the loop terminals. Within the tertiary structure of LA, the distance between C $^{\alpha}$

Keywords: α -Lactalbumin; Ca^{2+} -binding loop; Cyclic peptides; Circular dichroism; FTIR.

* Corresponding author. Tel.: +36 1 2090555; fax: +36 1 3722620; e-mail: majer@szerves.chem.elte.hu

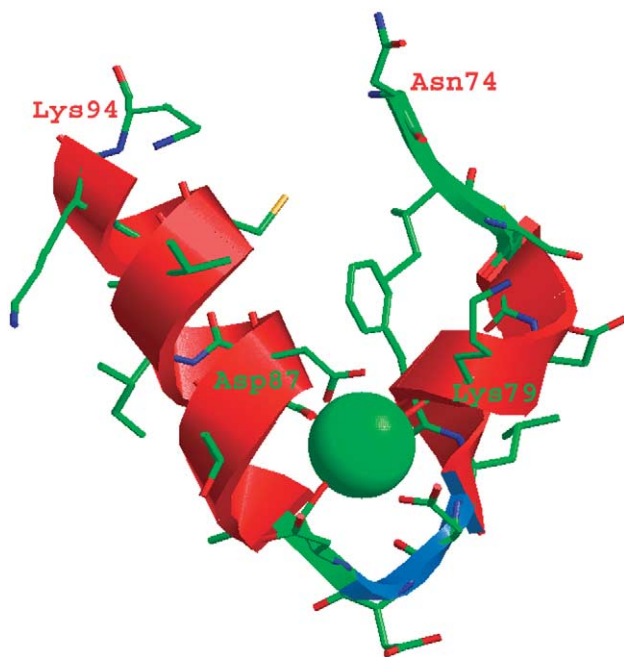


Figure 1. Calcium-binding site in α -lactalbumin from Asn⁷⁴ to Lys⁹⁴ [Protein Data Bank ID 1F6S, this picture was made by the use of RasTop (version 2.1) by Philippe Valadon (La Jolla, CA, USA)].²³

atoms of Lys⁷⁹ and C α atoms of Asp⁸⁸ is about 7.9 Å. All amino acids of the Ca²⁺-binding loop are strikingly well conserved among LAs of different species. The question arises to what extent individual amino acids that are not directly involved in the coordination of Ca²⁺ contribute to the binding affinity. The contribution of charged groups such as the positively charged Lys⁷⁹ and the negatively charged Asp⁸³ and Asp⁸⁴ residues is also of special interest. The side chain carboxylates of the latter Asp residues are not coordinated to Ca²⁺. However, they significantly increase the local charge density.

Idealized loops resemble a Greek omega (Ω). It is the conspicuous compactness of the loops, which allows their identification as a discrete entity in X-ray elucidated proteins. A loop structure is defined by the segment length (6–16 residues), the absence of regular secondary structures, and the distance between segment termini (<10 Å). Omega loops should be distinguished from disulfide-bridged ones. Loops are rigid structures but the shortness of their substructures suggests that they are chiroptically not well-defined conformations.⁸ It has been suggested that bicyclic peptides⁹ and longer linear peptides¹⁰ can mimic the three-dimensional structure of protein sites.

To answer the above question, we constructed model decapeptides mimicking the calcium-binding loop of LA with its ends connected with different linkers. Our first approach in the design of calcium-binding model compounds was simply to preserve the native sequence of LA loop in monocyclic analogues. Recognizing the importance of Lys side chain in calcium binding and/or in its influence on the local charge density, some

models without Lys were also synthesized. Alanine-containing models were designed for monitoring the role of the binding Asp residue (82, 87–88) **3d** and nonbinding Asp residue (83, 84) **3e** in coordination of the cation.

In the present study, we report the synthesis, structural characterization, and calcium binding of linear and cyclic model peptides (Table 1). Molecular mechanics (MM) was used to design the peptide models. At first the calcium-binding loop was calculated according to the X-ray structure of LA⁶ (Protein Data Bank ID: 1F6S). The minimum size of the linear model (**1**) was calculated to comprise 12 residues of the binding site of LA. The cyclic models **2–4** were calculated to contain 35–40 backbone atoms. Except for the Asp (D)- and Ala (A)-substituted models **3d** and **3e**, the cyclic models feature all five Asp residues that are present in the binding loop of LA. Disulfide, thioether, and lactam bridges were chosen to construct the ring.

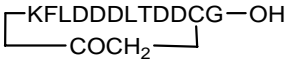
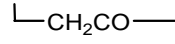
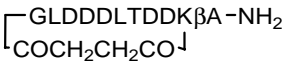
Circular dichroism (CD) and Fourier transform infrared (FTIR) spectroscopy were used to characterize the conformation and Ca²⁺-induced conformational transitions of the models. Cyclic peptides **3d–3f** were designed for clearing up the role of the binding (Asp⁸², Asp⁸⁷, and Asp⁸⁸) and nonbinding (Asp⁸³ and Asp⁸⁴) aspartic acid residues as well as the importance of Lys⁷⁹ in Ca²⁺ binding.

2. Results and discussion

2.1. Design and synthesis of peptides

On the basis of the results of MM calculation, we cut-out the Ca²⁺-binding loop of LA from Lys⁷⁹ to Asp⁸⁸. The Lys⁷⁹ side chain is not involved in Ca²⁺ binding⁶ (Protein Data Bank ID: 1F6S), and the modeling in vacuum showed the possibility of salt bridge formation between the ϵ -NH₂ of Lys and the β -COOH of Asp⁸⁷ or Asp⁸⁸. This feature could assist at the adoption of natural backbone conformation¹¹ and calcium binding. It is known that in protein, the mutation of Lys79 to alanine did not effect the Ca²⁺ binding but the mutant lost 50% of its tertiary structure; hence, this amino acid has a specific structural role in the protein.¹² Using different linkers—thioether (**2a–2b**), disulfide (**3a–3f**), and lactam bridge (**4**)—we investigated the effect of ring size and linker type on the secondary structure and the Ca-binding ability of cyclic peptides. Considering the synthetic routes two different connections were used: head-to-side chain (**2a** and **4**) and side chain-to-side chain (**2b** and **3a–3f**) cyclization. According to the X-ray data,⁶ the side chain of lysine is not involved in Ca²⁺ binding, only its backbone carbonyl oxygen. Therefore, we synthesized peptide **3c** (a serine analogue) to control the effect of side chain contribution on conformation and Ca²⁺ binding. The serine residue increases the hydrophilicity but no changes were observed in the conformation and Ca²⁺ binding of the peptide. Some peptides comprising lysine were prepared (**2a**, **3a**, **3d**, and **3e**) to establish the microenvironment of a possible salt bridge between the ϵ -NH₂ of Lys and the β -COOH of Asp⁸⁷ or Asp⁸⁸.

Table 1. Synthesis and analytical characterization of model peptides 1–4

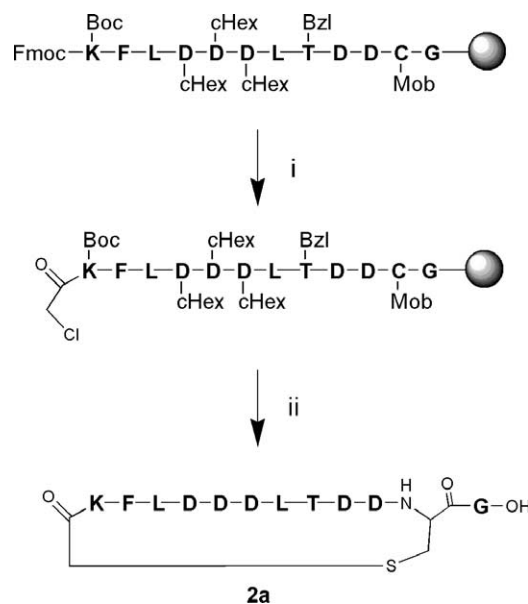
Peptides	Structure	MS data (M+H) ⁺ measured (calculated)	Retention time (min) ^a	Yield (%)
1	Ac-GKFLDDDLTDDG-OH	1352.1 (1351.6)	15.5	41
2a		1397.4 (1395.6)	15.9	10
2b	Ac-(CFLDDDLTDDK)G-NH ₂ 	1438.8 (1436.6)	17.0	7
3a	Ac-(CKFLDDDLTDDC)G-NH ₂	1497.9 (1497.6)	15.7	25
3b	Ac-(CFLDDDLTDDC)G-OH	1370.6 (1370.5)	18.0	19
3c	Ac-(CSFLDDDLTDDC)G-OH	1456.7 (1457.5)	14.9	22
3d	Ac-(CKFLDAAALTDDC)G-NH ₂	1410.0 (1409.6)	16.7	23
3e	Ac-(CKFLADDLTAAC)G-NH ₂	1366.3 (1365.6)	16.7	26
3f	Ac-(CFLDDDLTDDC)G-NH ₂	1369.9 (1369.0)	18.1	20
4		1259.0 (1257.5)	10.3	8

^a See Section 4 for details.

The contribution of Lys side chain resulted in a small change in the secondary structure in the case of peptides **3a** and **3f** (data not shown). The alanine-containing models were designed for monitoring the role of the binding Asp residues (82, 87–88) **3d** and nonbinding Asp residues (83–84) **3e** in the coordination of the cation.

The linear peptides were prepared by manual peptide synthesis on solid support using Boc/Bzl strategy; the side chain of Asp residues was protected as cyclohexyl (cHex) ester to minimize the aspartimide formation during the cleavages.¹³ The peptides were built in MBHA resin [(amino-[4-methylphenyl]methyl copolystyrene divinylbenzene) hydrochloride] except peptides **1**, **2a**, **3b**, and **3c**, where Merrifield resin (chloromethylpolystyrene-divinylbenzene) was used. The intramolecular cyclization to form a thioether bridge was achieved by two different methods (Schemes 1 and 2) and the yield after purification was 7–10%. The formation of the lactam bridge was performed with solid-phase cyclization (Scheme 4). After the cleavage of the side chain protecting group of lysine, the cyclization was performed by shaking the reactor for days. Disulfide bridge formation (Scheme 3) in two cysteine-containing peptides was easily achieved, according to the published results¹⁴ without difficulties. The cyclization was clearly monitored by HPLC (Fig. 2). The yield of the disulfide bridge containing cyclic peptides was ~24%, while lactam bridge was 8%.

Last step of solution-phase cyclization was the water evaporation in vacuo, and the purification procedure was the following: using HPLC with eluent A, the Tris-HCl (tris(hydroxymethyl)amino methane) was eliminated, while the cyclic peptide was eluted from the column with a gradient slope of 0.5% B/min. All

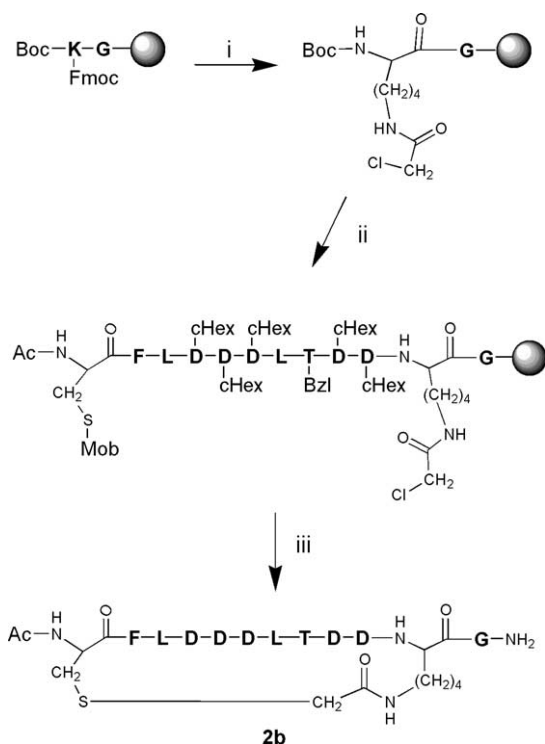


Scheme 1. Reagents and conditions for the synthesis of peptide **2a**: (i) (a) 2% DBU + 2% piperidine in DMF, (b) Cl-CH₂-CO-OPcp (3 equiv) in DMF; (ii) (a) 40% TFA in DCM, (b) HF, 1.5 h, -5 °C, *p*-cresol, thiocresol, (c) Tris-HCl buffer, 4–5 days.

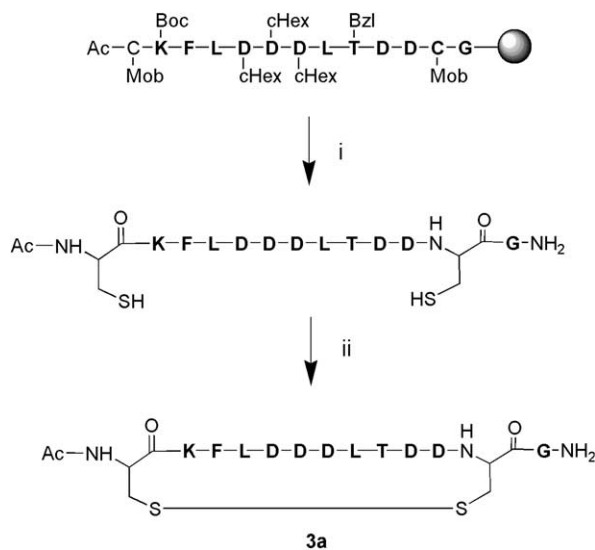
peptides were identified by MS and amino acid analyses (Table 1).

2.2. Spectroscopic studies

2.2.1. CD spectra of models 1–4. CD spectral parameters of linear (**1**) and bridged cyclic peptides (**2–4**) are summarized in Table 2. In the structure-promoting solvent TFE linear peptide **1** shows a spectrum marked by a strong positive band at 192 nm, a negative band at



Scheme 2. Reagents and conditions for the synthesis of peptide **2b**: (i) (a) 2% DBU + 2% piperidine in DMF, (b) Cl-CH₂-CO-OPcp (3 equiv) in DMF; (ii) (a) according to the Boc/Bzl protocol, (b) last Boc group cleavage followed by 5% acetic anhydride in pyridine; (iii) (a) HF, 1.5 h, -5 °C, *p*-cresol, thiocresol (b) Tris-HCl buffer, 4–5 days.



Scheme 3. Reagents and conditions for the synthesis of peptide **3a** (similar condition were applied for peptides **3b–3f**): (i) (a) 40% TFA in DCM, (b) HF, 1.5 h, -5 °C, *p*-cresol, thiocresol; (ii) Tris-HCl buffer, (pH 8.1–8.4) 4 days.

203 nm, and a negative $n\pi^*$ shoulder between 220 and 230 nm. This spectrum shows class C features and represents a mixture with high population of folded conformers (β -turns).¹⁵ In water or Tris-HCl buffer (pH 7), the spectrum changes significantly: the negative couplet is replaced by a strong negative band below 200 nm with

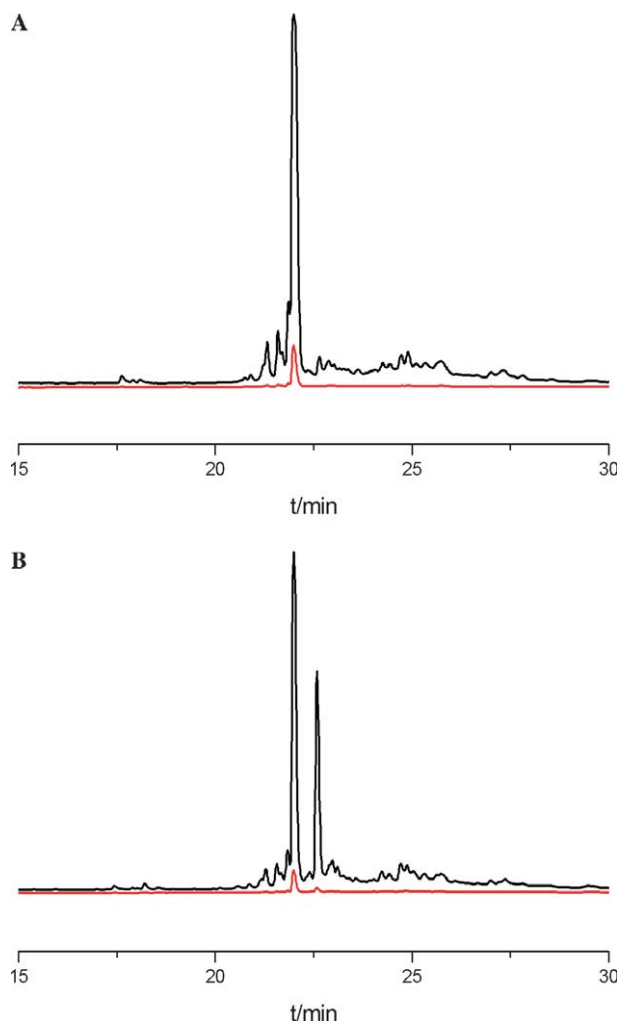


Figure 2. Analytical HPLC chromatogram of crude cyclopeptide **3a**, detected at 220 nm (black) and 260 nm (red). Peptide **3a** after 4 days cyclization (A) and cyclopeptide together with linear its linear precursor (B).

Table 2. CD data of model peptides

Peptides	Solvent	λ_{nm} ($[\theta]_{MR} \times 10^3$ (deg cm ² dmol ⁻¹))		
1	TFE	189 (9.30)	204 (-8.17)	218 (-7.05)
	H ₂ O	—	198 (-10.4)	218 (-3.82)
2a	TFE	184 (7.27)	201 (-10.14)	226 (-4.06)
	50% TFE	184 (4.40)	200 (-10.78)	229 (-3.33)
2b	TFE	187 (9.82)	203 (-8.82)	214 (-6.31)
	H ₂ O	182 (2.32)	199 (-10.37)	221 (-2.98)
2c	TFE	182 (9.73)	200 (-9.51)	217 (-5.33)
3a	TFE	184 (9.19)	202 (-11.80)	221 (-4.83)
	H ₂ O	183 (1.50)	200 (-11.84)	227 (-1.51)
3b	TFE	186 (8.98)	203 (-7.39)	218 (-4.88)
3c	TFE	185 (6.63)	202 (-7.74)	218 (-4.66)
3d	TFE	185 (5.35)	202 (-9.56)	222 (-4.80)
	H ₂ O	181 (-0.12)	200 (-11.61)	229 (-1.34)
3e	TFE	187 (2.34)	202 (-11.14)	220 (-3.78)
	H ₂ O	183 (-0.84)	200 (-10.77)	228 (-1.35)
3f	TFE	188 (10.94)	205 (-6.47)	219 (-4.91)
4	TFE	183 (8.76)	199 (-10.69)	218 (-3.61)
	50% TFE	185 (3.48)	200 (-12.95)	220 (-4.95)

a weak negative shoulder at 230 nm (class U spectrum). This spectrum is indicative of the predominance unordered (extended) conformers.

Cyclic peptides **2a**, **2b** (bridged by a CH_2CO group) and cyclic peptides **3a–3f** (comprising a disulfide bridge) also show CD spectra in TFE characterized by a negative $\pi\pi^*$ couplet and a negative $n\pi^*$ band (Table 2, Fig. 3) reflecting the presence of turn(s) within the macroring. Addition of less than 50% water to the solution in TFE does not have a significant spectral effect. The class C spectrum in TFE is replaced by a class U spectrum in water or in Tris buffer (pH 7). In the case of linear mid-size peptides, class C spectra reflect the presence of conformer population(s) of periodic ordered (α -helix or 3_{10} helix) or aperiodic ordered (type I or III β -turn) structures.¹⁵ Cyclic peptides cannot adopt longer helical stretches. Considering the amino acid sequence, ring size, and the presence of disulfide or other bridges, the adoption of turns is very probable. These turns are destroyed by water.

Compound **4** is unique within the series. There is a succinic acid bridge between its N-terminal glycine and the ε - NH_2 group of lysine residue acylating the β -alanine. Regardless of the enhanced flexibility of the macroring, the spectrum in TFE resembles the spectra of the other models in this solvent. The class C spectral features are preserved even in a 50% TFE–water mixture.

Neutralization of one or more aspartic acid carboxyl groups of **2b** resulted in a blue-shift of the negative couplet and a decrease of the relative intensity of the shoulder in the $n\pi^*$ spectral region. This is indicative of definite conformational changes without the loss of the comprised β -turn.

2.2.1.1. CD spectra in the presence of Ca^{2+} ions. CD-monitored Ca^{2+} -titration was performed on the disulfide-bridged cyclic peptides **3a**, **3d–3f**. The CD spectrum of the peptides shows more or less class C character (Fig. 3). Addition of Ca^{2+} gave rise to marked spectral shifts in the case of all cyclic models.

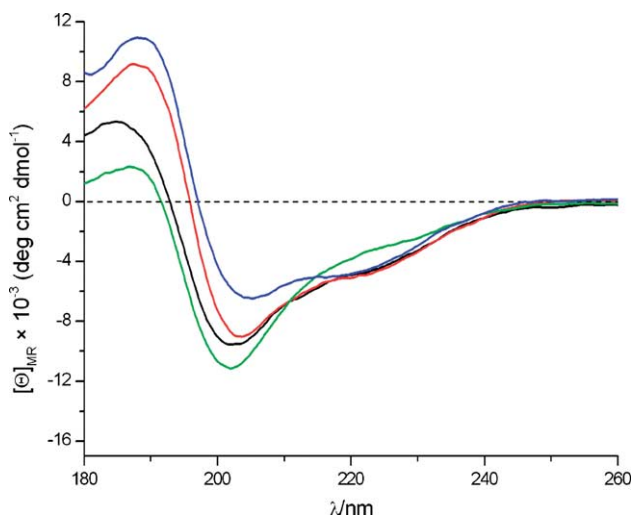
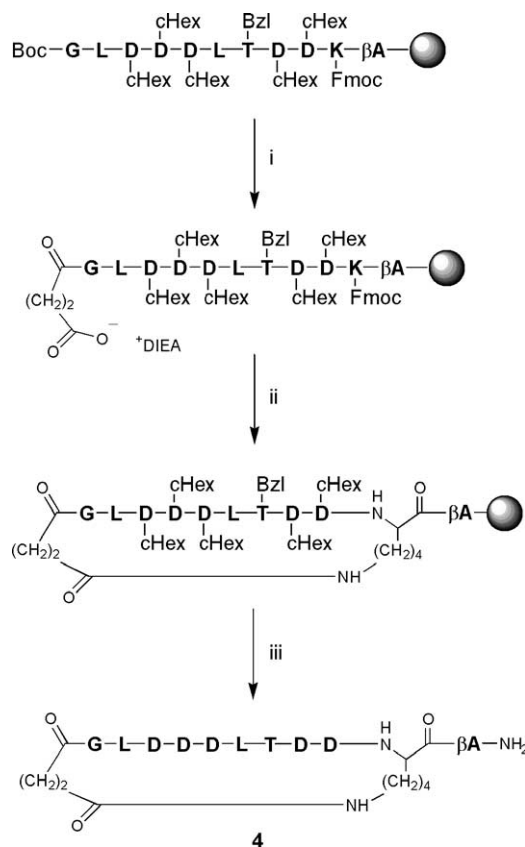


Figure 3. CD spectra of peptides **3a** (black), **3d** (red), **3e** (green), and **3f** (blue) in TFE.



Scheme 4. Reagents and conditions for the synthesis of peptide **4**: (i) (a) 40% TFA in DCM, (b) succinic anhydride (3 equiv), DIEA (3 equiv) in DMF; (ii) (a) 2% DBU + 2% piperidine in DMF, (b) DIC/HOBt (3 equiv) 3 days; (iii) HF, 1.5 h, 5 °C, *p*-cresol, thiocresol.

The CD spectra of **3a** with all five Asp residues of the binding loop changed differently below and above $\approx 0.5 \text{ Ca}^{2+}$ to peptide ratio. Less than 0.5 equiv Ca^{2+} caused an increase of the relative intensity of $n\pi^*$ band near 220 nm (Fig. 4). Contrary to this, **2a** also comprising five aspartic acid residues suffered marked spectral changes upon addition of ≥ 2 equiv of Ca^{2+} . Five equivalents of Ca^{2+} disrupted the negative couplet and induced a positive band at 217 nm (data not shown).

At $r_{\text{cat}} \approx 0.5$, the CD curve is indicative of a definite amount of β -strand structure.¹⁶ However, at the concentration of the peptide (0.35 mM), no aggregation can be observed. Above this ratio, the intensity of the $n\pi^*$ band in the spectrum decreased. At $r_{\text{cat}} = 5$, the $n\pi^*$ band almost vanished while the intensity of the negative $\pi\pi^*$ band appeared with increased intensity. Titration of **2a** and **2b**, also comprising five Asp residues, did not result at $r_{\text{cat}} \approx 0.5$ in a spectrum marked by a definite negative band near 220 nm (spectra not shown).

The CD spectra of the cyclic peptide **3d** changed gradually until $r_{\text{cat}} \approx 1.5$. Above this ratio, the spectra showed a nearly complete loss of the $n\pi^*$ band (Fig. 5). This is a sign of the binding of Ca^{2+} to backbone amide carbonyls after saturation of the inner binding site. The spectral behavior of **3e** is similar to that of **3d** until $r_{\text{cat}} = 1$. Increasing the molar excess of Ca^{2+} induces spectral

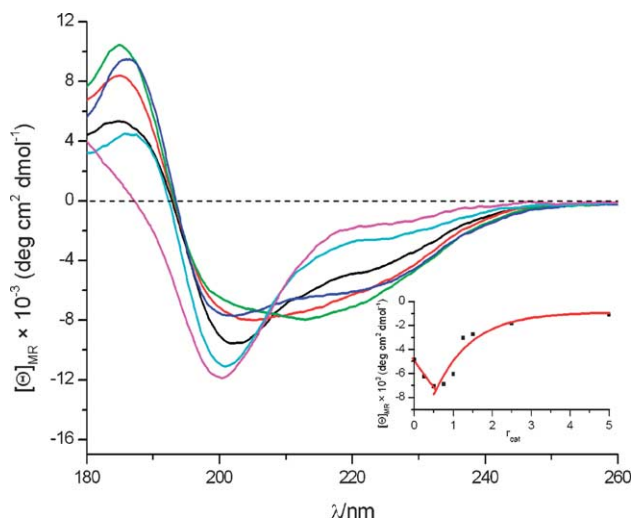


Figure 4. CD spectra of cyclic peptide **3a** (black) and the titration curves at $r_{\text{cat}} = 0.25$ (red), $r_{\text{cat}} = 0.5$ (green), $r_{\text{cat}} = 1$ (blue), $r_{\text{cat}} = 1.5$ (pale blue), and $r_{\text{cat}} = 2.5$ (purple) in TFE. The inset shows the dependence of the ellipticity at 220 nm as a function of r_{cat} .

changes in both the $\pi\pi^*$ and the $\pi\pi^*$ spectral regions (Fig. 6). The spectra at $r_{\text{cat}} \geq 1.5$ showed a positive band above 210 nm. The appearance of the positive band can be associated with Ca^{2+} binding to backbone carbonyls giving rise to marked conformational change. Features indicating the presence of β -strand conformation are not seen in the spectra of the Ca^{2+} complexes of cyclic peptides **3d** and **3e**.

The titration curves of **3f**, lacking Lys showed a gradual increase of the intensity of the negative $\pi\pi^*$ band until $r_{\text{cat}} \simeq 1$ but the $\pi\pi^*$ band did not change significantly. Above this, the intensity of the negative $\pi\pi^*$ decreased.

No time dependence was observed during CD-monitored Ca^{2+} titration of cyclic peptides **2** and **3**.

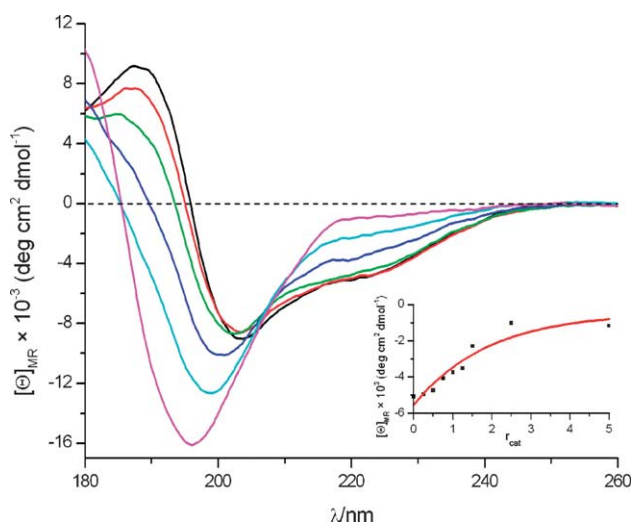


Figure 5. CD spectra of cyclic peptide **3d** (black) and the titration curves at $r_{\text{cat}} = 0.25$ (red), $r_{\text{cat}} = 0.5$ (green), $r_{\text{cat}} = 1$ (blue), $r_{\text{cat}} = 1.5$ (pale blue), and $r_{\text{cat}} = 2.5$ (purple) in TFE. The inset shows the dependence of the ellipticity at 220 nm as a function of r_{cat} .

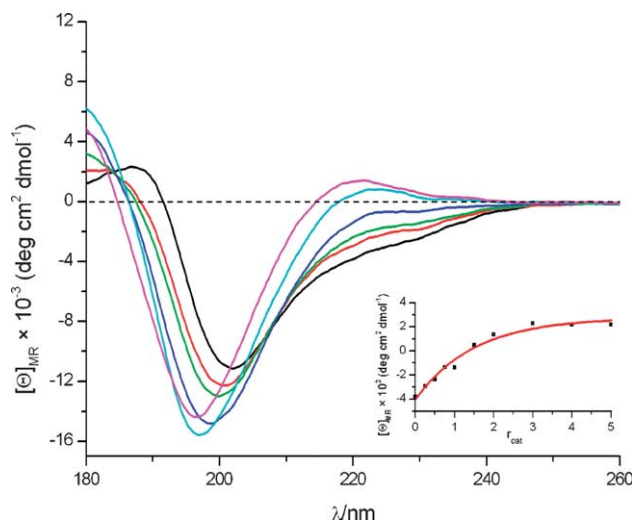


Figure 6. CD spectra of cyclic peptide **3e** (black) and the titration curves at $r_{\text{cat}} = 0.25$ (red), $r_{\text{cat}} = 0.5$ (green), $r_{\text{cat}} = 1$ (blue), $r_{\text{cat}} = 1.5$ (pale blue) and $r_{\text{cat}} = 2$ (purple) in TFE. The inset shows the dependence of the ellipticity at 220 nm as a function of r_{cat} .

2.2.2. FTIR spectroscopic studies. On the basis of the CD spectroscopic data on models **1–4**, FTIR spectroscopic measurements have been performed on the cyclic model **3a** and its alanine-substituted derivatives **3d** and **3e**. The spectra were taken in TFE in the $1800\text{--}1500\text{ cm}^{-1}$ spectral region, which is mainly composed of bands due to ν_{CO} (COOH), amide I, amide II, and ν_{as} (COO^-) vibrations but absorptions by the Lys (K) side chain [$\delta_{\text{asNH}_3^+}$ (K) and $\delta_{\text{sNH}_3^+}$ (K)] also give contribution to the spectrum. Some of the models are present as trifluoroacetate (TFA^-) salts. The strong ν_{as} (COO^-) band of TFA^- appears at $\sim 1675\text{ cm}^{-1}$. For comparison, the infrared spectrum of the des-lysine mode **3f** was also measured.

There are three main bands in the spectrum of the parent model **3a** at about 1725 cm^{-1} (ν_{CO}), 1675 cm^{-1} [amide I and ν_{as} (COO^-) of TFA^-], and 1540 cm^{-1} (amide II). The weak shoulders near ~ 1630 and $\sim 1600\text{ cm}^{-1}$ can be assigned to the absorption of side chains of Lys and Phe. The infrared spectra of **3a**, **3d**, and **3e** are similar except that the relative intensity of the ν_{CO} band is smaller in the spectra of **3d** and especially **3e** comprising three and two Asp residues, respectively. The positions and decreased intensity of the amide I band in the spectrum of **3f** comprising no lysine and bound TFA^- is in agreement with expectation (Fig. 7). The shape and deconvolution of the amide I bands do not give information about the secondary structure of the ring comprising 38 backbone atoms. The low wavenumber shoulder of the amide I band may be a sign of the spectral contribution of turn(s). The amide I component band of the acceptor CO of intramolecular H-bond(s) of β - and γ -turns was suggested to appear near 1640 and 1620 cm^{-1} , respectively.¹⁷

2.2.2.1. FTIR spectra in the presence of Ca^{2+} ions. The cyclic peptide **3a** comprising five Asp residues resulted in a turbid solution and separation of a precipitate in the presence of 0.5–1.5 equiv Ca^{2+} [c_p (peptide

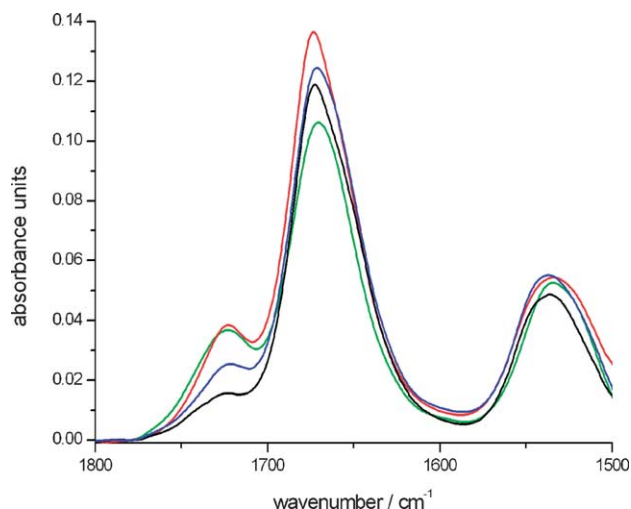


Figure 7. FTIR spectra of peptides **3a** (red), **3d** (blue), **3e** (black), and **3f** (green) obtained in TFE.

concentration) = 1.5 mM in TFE] which obscured the measurement. Models **3d** and **3e** comprising no lysine showed no precipitation in the presence of Ca^{2+} . (A weak tendency for aggregation was observed in the case of **3f** not comprising Lys. The presence of lysine appears to promote aggregation even at lower Ca^{2+} ion concentrations.) It was observed, however, that the spectra show differences depending on the time passed after dissolving the peptide in the TFE solution of the calcium salt. Therefore the complexation of Ca^{2+} was followed in time. The spectra at $r_{\text{cat}} = 0.5$ showed definite time dependence. The amide I band became constant after 60 min while the ν_{CO} (COOH) and amide II plus ν_{as} (COO^-) regions changed for a longer time.

The intensity decrease of the ν_{CO} band was accompanied by an increase and broadening of the band below $\sim 1600 \text{ cm}^{-1}$ (strong high wavenumber shoulder at $\sim 1585 \text{ cm}^{-1}$) as a sign of the decrease of the number of COOH and increase of the Ca^{2+} -binding COO^- groups.

The cyclic peptide **3d** features the three Asp residues that in LA are involved in Ca^{2+} binding according to X-ray crystallography.⁶ In the presence of Ca^{2+} at $r_{\text{cat}} = 1$ the spectra showed time dependence but only until $\sim 90 \text{ min}$ (Fig. 8). The spectra are similar to that of **3f** (not shown). Interestingly, at $r_{\text{cat}} = 1$ and 1.5, a component band appeared at $\sim 1605 \text{ cm}^{-1}$ reflecting the presence of a COO^- group binding Ca^{2+} in a unidentate manner, which is expected to increase the frequency of the ν_{as} (COO^-) band.¹⁸

Cyclic peptide **3e** comprises only two Asp residues that in LA are not coordinated to Ca^{2+} . Regardless of the Ca^{2+} to peptide ratio, the spectra changed in time until $\sim 60 \text{ min}$ (Fig. 9). After reaching the complex equilibrium, the spectra showed two characteristic features: a definite shoulder at $\sim 1700 \text{ cm}^{-1}$ in the ν_{CO} region and another one at $\sim 1590 \text{ cm}^{-1}$. It is reasonable to suppose that the shoulder at $\sim 1700 \text{ cm}^{-1}$ indicates the formation

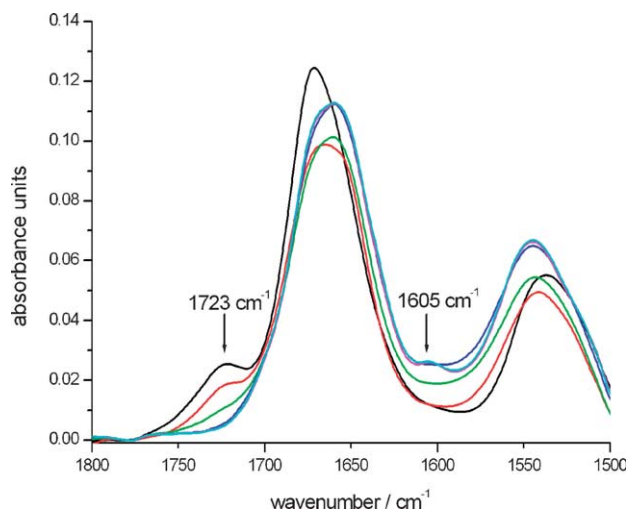


Figure 8. FTIR spectra of cyclic peptide **3d** in TFE (black) and the curves at 0 min (red), after 30 min (green), after 1 h (blue), and after 1.5 h (purple) in the presence of Ca^{2+} ions at $r_{\text{cat}} = 1$.

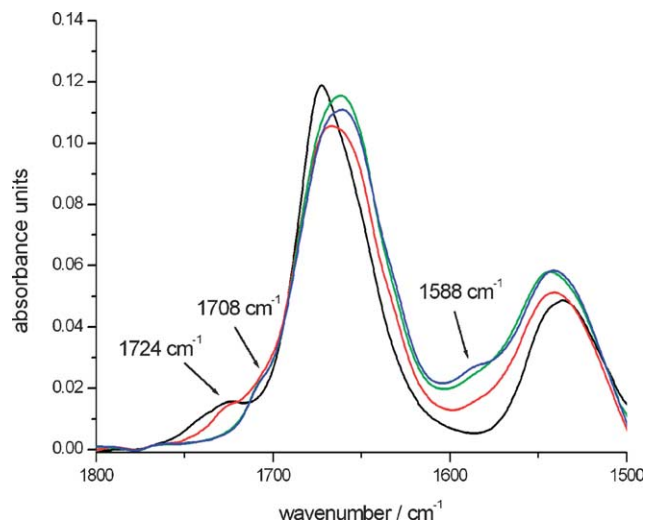
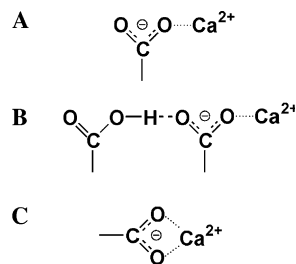


Figure 9. FTIR spectra of cyclic peptide **3e** in TFE (black) and the curves at 0 min (red), after 30 min (green), and after 1 h (blue) in the presence of Ca^{2+} ions at $r_{\text{cat}} = 1$.



Scheme 5. Unidentate (A), bridged (B), and bidentate (C) metal-ion binding systems.

of a Ca^{2+} -binding H-bonded system participated by the side chain COO^- functions of two neighboring Asp residues in which the proton involved in H-bond acts as a bridging 'pseudo metal' ion (Scheme 5). The

low-wavenumber component at $\sim 1585\text{ cm}^{-1}$ can be assigned to the $\nu_{\text{as}}(\text{COO}^-)$ of the H-bond acceptor aspartate side chain binding Ca^{2+} ion.

3. Conclusion

One linear (**1**) and a series of cyclic peptides (**2–4**) were designed and synthesized for modeling the elbow-type Ca^{2+} -binding loop of LA. Different linkers were used to form a monocyclic system in models **2–4** with roughly the same inner size of the ring (the distance between the C^α atoms of Lys⁷⁹ and Asp⁸⁸ is about 7.9 Å).

The structural features of synthetic peptides and their Ca^{2+} -binding properties were investigated in solution by CD and FTIR spectroscopy. In TFE, both the linear model and the cyclic ones were found to have a class C-type CD spectrum reflecting the presence of folded (turn) conformers.¹⁵ No marked differences were seen in the spectra of cyclic models having different bridges. In water, the CD curves show a strong negative band below 200 nm as a sign of the presence of unordered (extended) conformers. No conformational transition was observed upon changes of pH in the range of 3.5–11.

In analogy with other synthetic peptides mimicking the calcium-binding loop, no evidence of Ca^{2+} binding in water at various pH values (pH 3.5–11) and in a TFE/ H_2O 1:1 mixture was observed. Apparently, the Ca^{2+} affinity of the binding site of models **1–4** is not strong enough to remove (or partially remove) the water molecules surrounding the Ca^{2+} ion and undergo marked backbone conformational transitions resulting in a discernible CD spectral effect. In neat TFE, the cyclic peptides showed marked spectral changes in the presence of Ca^{2+} . The effect of Ca^{2+} was dependent on the structure and concentration of the model and the Ca^{2+} to peptide ratio. Above $r_{\text{cat}} \approx 2$, the negative couplet in the $\pi\pi^*$ region was replaced by a blue-shifted negative band indicating chain extension that is unfolding of the turn(s) within the macroring. The decreased intensity of the negative $n\pi^*$ band or the appearance of a positive band between 215 and 230 nm is indicative of the binding of Ca^{2+} not only to the side chains of Asp but also to amide carbonyl(s) of the peptide backbone.

FTIR spectroscopy proved to be more informative. Comparative infrared studies have been performed on the cyclic model **3a** and its Ala for Asp substituted derivatives **3d** and **3e**. Unfortunately, even at a $r_{\text{cat}} = 0.5$ Ca^{2+} ions caused precipitation of the parent peptide **3a**. Precipitation was not observed for the Ala-containing models **3d** and **3e**.

Titration with Ca^{2+} gave rise to a decrease of the intensity of the $\nu_{\text{CO}}(\text{COOH})$ band and an increase of the $\nu_{\text{as}}(\text{COO}^-)$ band of Asp residue(s). The Ala for Asp substitution of LA (**3d** and **3e**, respectively) enabled us to evaluate the relative importance of Asp residues in the Ca^{2+} -binding loop of LA. The time dependence of the spectral changes in the amide I, $\nu_{\text{CO}}(\text{COOH})$, and $\nu_{\text{as}}(\text{COO}^-)$ spectral regions was different. The shape of the broad

amide I band showed no more change after ~ 60 min. Contrary to this, the deprotonation of the side chain COOH group(s) and formation of the final coordination sphere of Ca^{2+} took more time.

In aqueous solution at pH ~ 7 , the Asp side chains are deprotonated. In TFE solution, the majority of Asp residues was protonated. TFE is a unique solvent due to its lower dielectric constant and the presence of the noninteractive, repulsive character of the trifluoromethyl group.^{19,20} This solvent was suggested to mimic biological binding sites that are buried or less accessible to water. In TFE, Ca^{2+} binding must be preceded by deprotonation of the Asp side chain(s) involved in the coordination of Ca^{2+} . On the basis of the relatively low rate of deprotonation (~ 90 min) in the case of both **3d** and **3e**, the replacement of protons by Ca^{2+} appears to be a favorable but slow process in TFE. The cost of Ca^{2+} binding is that the solvent becomes acidic: the lost protons are likely bound to water molecules that are present in small amount in TFE solution. As shown in Figures 8 and 9, the spectral patterns of the Ca^{2+} complex of **3d** and **3e** are different. In the complex of **3d**, comprising the binding Asp residues of LA, the Ca^{2+} ion is coordinated by the COO^- groups of all three Asp. In the complex of **3e**, the two neighboring Asp side chains form a bridged Ca^{2+} -binding system (Scheme 5). Using models **3d** and **3e** comprising the binding and nonbinding Asp residues, respectively, FTIR spectroscopy revealed the crucial role of the distal Asp residue in the binding site of LA.

4. Experimental

4.1. General methods

The amino acids were represented by three- and one letter code. Protected amino acids [Boc-Gly-OH, Boc- β Ala-OH, Boc-Cys(Mob)-OH, Boc-Asp(OcHex)-OH, Boc-Leu-OH, Boc-Lys(Fmoc)-OH, Boc-Thr(Bzl)-OH, Boc-Phe-OH, (Fmoc = 9-fluorenylmethoxycarbonyl, Mob = *para*-methoxybenzyl)], solvents, and reagents were purchased from Reanal Co. (Hungary), Novabiochem, and Fluka. The solvents for the spectroscopic studies were TFE (Aldrich, NMR grade) and double distilled water.

Circular dichroism measurements were performed on Jasco Dichrograph J-810 at room temperature in quartz cell with 0.02 cm path length. The spectra were averaged of five scans in the region 185 and 300 nm. The concentration of peptide was 0.5–1 mg/ml. CD band intensities are expressed in mean residue ellipticity ($[\theta]_{\text{MR}}$, deg cm^2/dmol).

Ca^{2+} stock solution (21 mM) was prepared from $\text{Ca}(\text{ClO}_4)_2 \cdot 4\text{H}_2\text{O}$ (Aldrich, 99%) in TFE. Titrations were performed until $r_{\text{cat}} = 10$, where $r_{\text{cat}} = [\text{Ca}^{2+}]/[\text{peptide}]$.

FTIR spectra were recorded on a Bruker Equinox 55 spectrometer at room temperature in a CaF_2 cell of 0.02 cm path length. The peptide concentration in

TFE was 1.5 mmol in each measurement and titration was performed in a solution of $\text{Ca}(\text{ClO}_4)_2 \cdot 4\text{H}_2\text{O}$ in TFE ($r_{\text{cat}} = 0.5, 1, \text{ and } 1.5$). The spectra were corrected with the background.

Analytical HPLC was carried out on a Jasco-HPLC instrument with Alltima column (C-18, 5 μm , WP, $250 \times 4.6 \text{ mm}$) using 0.1% TFA in water (A) and 0.08% TFA in acetonitrile (B) as eluents. Gradient: 5–95% eluent B over 30 min. Flow rate was 1 ml/min. The preparative HPLC was performed with Knauer instrumentation with preparative pump-head using Alltima column (C-18, 5 μm , WP, $250 \times 22 \text{ mm}$), and for semipreparative purification, Vydac column (C-18, 10 μm , 300Å, $250 \times 10 \text{ mm}$) and an analytical pump-head were used with the above written eluents.

HyperChem 6.0 program was adopted for the MM calculation of the model cyclic peptides, using the conformational search module.²¹ The structure optimizations were performed in vacuum using Polak-Ribiere algorithm and AMBER force field. The amide groups were inserted in the *trans*-form as restraints to avoid the formation of the *cis*-amide groups.

4.1.1. Peptide synthesis and purification. Linear peptide and peptide derivatives were synthesized using Merrifield resin (1.0 mmol/g) and MBHA resin (0.98 and 0.61 mmol/g), pre-swelling 5–6 h in DCM. The first Boc amino acid was attached to the Merrifield resin as a cesium salt: 0.5 g Boc-Gly-OH was dissolved in 2.5 ml EtOH + 1 ml H_2O and the pH was adjusted to 7 with 2 M aq Cs_2CO_3 . The solution was evaporated in vacuo to dryness and eliminated water by evaporation of EtOH and benzene from the resin. Boc-Gly-OCs salt (0.31 g, 1 mM) was added to the suspended resin (0.5 g) and shaken for 24 h at 50 °C. The resin was washed with 3 \times DMF, 3 \times MeOH, 3 \times DMF/ H_2O , 3 \times DMF, and 3 \times MeOH. The coupling was monitored by elemental analysis.

In the case of MBHA resin, the attachment of the first amino acid was performed with the DIC/HOBt (1,3-diisopropylcarbodiimide/1-hydroxybenzotriazole) coupling protocol (5 equiv amino acid, 5 equiv HOBt, 5 equiv DIC for 3 h at room temperature). Deprotection was carried out in 40% TFA/DCM for 20 min followed 5 times washing procedure by DCM and neutralization by DIEA for 5 min. Coupling was performed according to the Boc/Bzl (*tert*-butoxycarbonyl/benzyl) protocol²² in DCM using DIC/HOBt (3 equiv) for 40 min. The coupling was monitored by Kaiser test. The side chain of Boc-Asp was protected with *c*Hex group. After the cleavage of the last BOC group from N-terminal, the acetylation was performed with acetic acid anhydride/DIC (5 equiv/5 equiv) in DMF solution. The peptides with free thiol groups were cleaved from the resin by liquid hydrogen fluoride (HF) (10 ml/1 g resin) in the presence of scavengers (peptide:*p*-cresol:thiocresol = 1:1.0:0.1 g) for 1.5 h at –5 °C. After cleavage procedure, the resin was washed with 150 ml ether and treated with 10 ml 40% acetic acid/water, 10 ml 20% acetic acid/water and water. The water phase solutions were diluted about to 5% acetic acid solution and lyophilized.

4.2. Synthesis

4.2.1. Preparation of Ac-Gly-Lys-Phe-Leu-Asp-Asp-Asp-Leu-Thr-Asp-Asp-Gly-OH (1). The synthesis was performed on Merrifield resin (0.3 g, 0.29 mmol). The yield was 41% (162 mg). Analytical HPLC t_R (retention time): 15.5 min. ESI-MS $[\text{M}+\text{H}^+]$: 1352.1 (calcd 1351.6, $\text{C}_{57}\text{H}_{85}\text{N}_{13}\text{O}_{25}$). Amino acid analysis: Asp 4.94 (5), Gly 0.90 (1), Leu 1.90 (2), Lys 0.88 (1), Phe 0.95 (1), and Thr 0.93 (1). The purity of the peptide was 97% according to HPLC.

4.2.2. Preparation of Cl-CH₂-CO-Lys-Phe-Leu-Asp-Asp-Asp-Leu-Thr-Asp-Asp-Cys-Gly-OH (precursor of 2a). The synthesis was performed on Merrifield resin (0.42 g, 0.42 mmol) and running with Boc/Bzl strategy. The last coupling was performed with Fmoc-Lys(Boc)-OH (3 equiv) by the method described above. For Fmoc cleavage 2% DBU (1,8-diazabicyclo[5.4.0]undec-7-ene)/2% piperidine/DMF solution (10 ml) was added to the peptidyl polymer until 20 min. After the washing procedure (3 \times DMF), ClAc-OPcp (chloroacetic acid penta-chlorophenyl ester) (2 ml, 1.2 M, 3 equiv) in DMF was added. The resin was shaken until 2 h, the negative Kaiser test showed the success of coupling. The peptidyl polymer was washed with 3 \times DMF, 3 \times DCM, 3 \times MeOH and diethyl ether. The dried resin was cleaved from resin performed by HF. The yield of the crude linear peptide was 62% (350 mg).

4.2.3. Cyclization of Cl-CH₂-CO-Lys-Phe-Leu-Asp-Asp-Asp-Leu-Thr-Asp-Asp-Cys-Gly-OH (precursor of 2a). 150 mg crude linear precursor was dissolved in Tris-HCl (160 ml, 0.97 g Tris + 3.50 ml 1 M HCl; pH 8.1–8.4) buffer in a stocked system (protecting from air) and was slowly stirred until 4 days. The water was evaporated and the cyclopeptide **2a** purified with preparative HPLC. The yield: 10% (14 mg). Analytical HPLC t_R 15.9 min. ESI-MS $[\text{M}+\text{H}^+]$: 1397.4 (calcd 1395.6, $\text{C}_{58}\text{H}_{85}\text{N}_{13}\text{O}_{25}\text{S}$). Amino acid analysis: Asp 4.94 (5), Gly 0.92 (1), Leu 1.90 (2), Lys 0.91 (1), Phe 0.95 (1), and Thr 0.96 (1). The purity of the cyclopeptide **2a** was 95% according to HPLC.

4.2.4. Preparation of Ac-Cys-Phe-Leu-Asp-Asp-Asp-Leu-Thr-Asp-Asp-Lys(Cl-CH₂-CO)-Gly-NH₂ (precursor of 2b). The synthesis was performed on MBHA resin (0.5 g, 0.49 mmol). The resin-bounded dipeptide [Boc-Lys(Fmoc)-Gly-resin] was treated with 2% DBU/2% piperidine/DMF solution (10 ml) for 20 min to cleave Fmoc group and washed with 3 \times DMF. The ClAc-OPcp in DMF solution (2 ml, 1.2 M, 3 equiv) was added to the peptidyl resin for 2 h, and the coupling was monitored by Kaiser test. The solid-phase peptide synthesis was continued with Boc protocol. After the cleavage from the resin, the yield of the crude linear peptide was 53% (210 mg).

4.2.5. Cyclization of Ac-Cys-Phe-Leu-Asp-Asp-Asp-Leu-Thr-Asp-Asp-Lys(Cl-CH₂-CO)-Gly-NH₂. The conditions of the cyclization were similar as **2a**. Cyclopeptide **2b** purified with preparative HPLC. The yield: 7% (13 mg). Analytical HPLC t_R : 17.0 min. ESI-MS $[\text{M}+\text{H}^+]$: 1438.8 (calcd 1436.6, $\text{C}_{60}\text{H}_{88}\text{N}_{14}\text{O}_{25}\text{S}$). Amino

acid analysis: Asp 4.85 (5), Gly 0.95 (1), Leu 1.89 (2), Phe 0.96 (1), and Thr 0.94 (1). The purity of the cyclopeptide **2b** was 94% according to HPLC.

4.2.6. Preparation of linear precursors of the peptides 3a–3f. The synthesis was performed on MBHA resin (0.5 g, 0.61 mmol/g). After the cleavage of the peptides from resin, the yield of the crude product was 78% (360 mg) for **3a**, 78% (338 mg) for **3d**, 73% (243 mg) for **3e**, and 57% (237 mg) for **3f**.

In the case of **3b** and **3c**, the synthesis was performed in Merrifield resin (0.5 g, 0.98 mmol/g). After the cleavage from resin, the yield of the crude linear peptide was 34% (228 mg) for **3b** and 29% (208 mg) for **3c**.

4.2.7. Cyclization of disulfide bridge containing peptides.

4.2.7.1. General method. The linear peptides were dissolved in Tris–HCl (1 l, 6.05 g Tris + 21.9 ml 1 M HCl; pH 8.1–8.4) buffer. The concentration was 0.07 mg/l. The solution was stirred until 3 days in an opened flask. The oxidation achieved by entered compressed air, and monitored by HPLC.

4.2.7.1.1. Peptide 3a. The yield: 25% (17.5 mg). Analytical HPLC t_R : 15.7 min. ESI-MS $[M+H]^+$: 1497.9 (calcd 1497.6, $C_{61}H_{91}N_{15}O_{25}S_2$). Amino acid analysis: Asp 4.90 (5), Gly 0.96 (1), Leu 1.92 (2), Phe 0.96 (1), and Thr 0.94 (1). The purity of the cyclopeptide was 96% according to HPLC.

4.2.7.1.2. Peptide 3b. The yield: 19% (13.0 mg). Analytical HPLC t_R : 18.0 min. ESI-MS $[M+H]^+$: 1370.6 (calcd 1370.5, $C_{55}H_{78}N_{12}O_{25}S_2$). Amino acid analysis: Asp 4.93 (5), Gly 0.95 (1), Leu 1.92 (2), Phe 0.95 (1), and Thr 0.95 (1). The purity of the cyclopeptide was 94% according to HPLC.

4.2.7.1.3. Peptide 3c. The yield: 22% (15.4 mg). Analytical HPLC t_R : 14.9 min. ESI-MS $[M+H]^+$: 1456.7 (calcd 1457.5, $C_{58}H_{83}N_{13}O_{27}S_2$). Amino acid analysis: Asp 4.93 (5), Gly 1.01 (1), Leu 2.02 (2), Phe 0.88 (1), and Thr 0.99 (1). The purity of the cyclopeptide was 93% according to HPLC.

4.2.7.1.4. Peptide 3d. The yield: 23% (16.1 mg). Analytical HPLC t_R : 16.7 min. ESI-MS $[M+H]^+$: 1410.0 (calcd 1409.6, $C_{59}H_{91}N_{15}O_{21}S_2$). Amino acid analysis: Ala 2.00 (2), Asp 2.75 (3), Gly 0.90 (1), Leu 1.74 (2), Phe 0.88 (1), and Thr 0.82 (1). The purity of the cyclopeptide was 98% according to HPLC.

4.2.7.1.5. Peptide 3e. The yield: 26% (18.2 mg). Analytical HPLC t_R : 16.7 min. ESI-MS $[M+H]^+$: 1366.3 (calcd 1365.6, $C_{58}H_{91}N_{15}O_{19}S_2$). Amino acid analysis: Ala 2.88 (3), Asp 1.82 (2), Gly 0.96 (1), Leu 1.90 (2), Phe 0.88 (1), and Thr 0.90 (1). The purity of the cyclopeptide was 97% according to HPLC.

4.2.7.1.6. Peptide 3f. The yield: 20% (14.0 mg). Analytical HPLC t_R : 18.1 min. ESI-MS $[M+H]^+$: 1369.9 (calcd 1369.5, $C_{55}H_{79}N_{13}O_{24}S_2$). Amino acid analysis: Asp 4.88 (5), Gly 0.90 (1), Leu 1.89 (2), Phe 0.91 (1), and Thr 0.90 (1). The purity of the cyclopeptide was 93% according to HPLC.

4.2.8. Preparation of cyclic peptide 4 by solid-phase cyclization. The synthesis was performed on MBHA resin (0.1 g, 0.098 mmol), where Lys side chain was

protected by Fmoc group. After the cleavage of the Boc protecting group from Gly, the resin was washed with 3× DMF. The solution of succinic anhydride (88.4 mg, 0.88 mmol) and DIEA (*N,N*-diisopropylethylamine) (151 μ l, 0.88 mmol) in DMF was added to the peptidyl resin for 30 min, and the coupling was followed by the Kaiser test. The resin was washed with 3× DMF, 3× DCM, 3× DMF and treated with 2% DBU 2% piperidine in DMF solution (10 ml) for 3 + 17 min. (Fmoc cleavage). The resin was suspended in DMF and cyclization was carried out with solution of DIC (168 μ l, 0.88 mmol) and HOBt (119 mg, 0.88 mmol) in 3 ml DMF and the mixture was stirred for 3 days. The coupling reagents were refreshed daily. After the cleavage from the resin, the yield of the cyclopeptide **4** was 8% (10 mg). Analytical HPLC conditions: Vydac 150 × 4.6 mm column (C-18, 5 μ m, WP), gradient: 5% B until 5 min followed by 5%–65% eluent B over 45 min. Flow rate was 1.2 ml/min. Retention time: 10.3 min. FAB-MS: 1259 (calcd 1257.5, $C_{51}H_{79}N_{13}O_{24}$). The purity of the cyclopeptide was 92% according to HPLC.

Acknowledgments

This work was supported by the Hungarian Research Fund [OTKA Grants T037719 (Zs.M.), T047186 (E.V.), T049792 (M.H.)], FWO-Flanders G-0180-03 (I.H.), the Bilateral Scientific Cooperation (B-16/04), and the János Bolyai Research Scholarship of the Hungarian Academy of Science (E.V.).

References and notes

- Hiraoka, Y.; Segawa, T.; Kuwajima, K.; Sugai, S.; Murai, N. *Biochem. Biophys. Res. Commun.* **1980**, *95*, 1098–1104.
- Kronman, M. J. *Crit. Rev. Biochem. Mol. Biol.* **1989**, *24*, 565–667.
- Kuwajima, K. *FASEB J.* **1996**, *10*, 102–109.
- Kuwajima, K.; Ikeguchi, M.; Sugawara, T.; Hiraoka, Y.; Sugai, S. *Biochemistry-U.S.* **1990**, *29*, 8240–8249.
- Stuart, D. I.; Acharya, K. R.; Walker, N. P. C.; Smith, S. G.; Lewis, M.; Phillips, D. C. *Nature* **1986**, *324*, 84–87.
- Chrysina, E. D.; Brew, K.; Acharya, K. R. *J. Biol. Chem.* **2000**, *275*, 37021–37029.
- Kretsinger, R. H. *CRC Crit. Rev. Biochem. Mol.* **1980**, *8*, 119–174.
- Leszczynski, J. F.; Rose, G. D. *Science* **1986**, *234*, 849–855.
- Oliva, R.; Falcigno, L.; D'Auria, G.; Saviano, M.; Paolillo, L.; Ansanelli, G.; Zanotti, G. *Biopolymers* **2000**, *53*, 581–595.
- Kuhlman, B.; Boice, J. A.; Wu, W. J.; Fairman, R.; Raleigh, D. P. *Biochemistry* **1997**, *36*, 4607–4615.
- Smith, J. S.; Scholtz, J. M. *Biochemistry* **1998**, *37*, 33–40.
- Anderson, P. J.; Brooks, C. L.; Berliner, L. J. *Biochemistry* **1997**, *36*, 11648–11654.
- Tam, J. P.; Riemen, M. W.; Merrifield, R. B. *Peptide Res.* **1988**, *1*, 6.
- Andreu, D.; Albericio, F.; Solé, N. A.; Munson, M. C.; Ferrer, M.; Barany, G. *Methods in Molecular Biology In Peptide Synthesis Protocols*; Humana: Totowa, 1994; Vol. 35, pp 91–169.

15. Perczel, A.; Hollósi, M.. In *Circular Dichroism and the Conformational Analysis of Biomolecules*; Fasman, G. D., Ed.; Plenum: New York, 1996, pp 285–380.
16. Fasman, G. D. *Circular Dichroism and the Conformational Analysis of Biomolecules*; Plenum: New York, 1996.
17. Vass, E.; Hollósi, M.; Besson, F.; Buchet, R. *Chem. Rev.* **2003**, *103*, 1917–1954.
18. Deacon, G. B.; Phillips, R. J. *Coord. Chem. Rev.* **1980**, *33*, 227–250.
19. Nelson, J. W.; Kallenbach, N. R. *Proteins* **1986**, *2*, 211.
20. Jackson, M.; Mantsch, H. H. *Biochim. Biophys. Acta* **1992**, *1118*, 139–143.
21. HyperChem(TM) Professional; 6.0 ed.; Hypercube: Gainesville, Florida 32601, USA, 1999.
22. Stewart, J. M.; Young, J. D. *Solid Phase Peptide Synthesis*; Pierce Chemical Company: Rockford, Illinois, 1984.
23. Bernstein, H. J. *Trends Biochem. Sci. (TIBS)* **2000**, *25*, 453–455.